

PPPL-5261

## Recent Advances Towards a Lithium Vapor Box Divertor

R.J. Goldston, A. Hakim, G.W. Hammett, M.A. Jaworski, J. Schwartz

July 2016



Prepared for the U.S. Department of Energy under Contract DE-AC02-09CH11466.

# Princeton Plasma Physics Laboratory

## Report Disclaimers

---

### Full Legal Disclaimer

This report was prepared as an account of work sponsored by an agency of the United States Government. Neither the United States Government nor any agency thereof, nor any of their employees, nor any of their contractors, subcontractors or their employees, makes any warranty, express or implied, or assumes any legal liability or responsibility for the accuracy, completeness, or any third party's use or the results of such use of any information, apparatus, product, or process disclosed, or represents that its use would not infringe privately owned rights. Reference herein to any specific commercial product, process, or service by trade name, trademark, manufacturer, or otherwise, does not necessarily constitute or imply its endorsement, recommendation, or favoring by the United States Government or any agency thereof or its contractors or subcontractors. The views and opinions of authors expressed herein do not necessarily state or reflect those of the United States Government or any agency thereof.

### Trademark Disclaimer

Reference herein to any specific commercial product, process, or service by trade name, trademark, manufacturer, or otherwise, does not necessarily constitute or imply its endorsement, recommendation, or favoring by the United States Government or any agency thereof or its contractors or subcontractors.

---

## PPPL Report Availability

### Princeton Plasma Physics Laboratory:

<http://www.pppl.gov/techreports.cfm>

### Office of Scientific and Technical Information (OSTI):

<http://www.osti.gov/scitech/>

---

### Related Links:

[U.S. Department of Energy](#)

[U.S. Department of Energy Office of Science](#)

[U.S. Department of Energy Office of Fusion Energy Sciences](#)

## Recent Advances Towards a Lithium Vapor Box Divertor

R.J. Goldston, A. Hakim, G.W. Hammett, M.A. Jaworski, J. Schwartz  
Princeton Plasma Physics Laboratory

### Abstract

Fusion power plants are likely to require near complete detachment of the divertor plasma from the divertor target plates, in order to have both acceptable heat flux at the target to avoid prompt damage and acceptable plasma temperature at the target surface, to minimize long-term erosion. However hydrogenic and impurity puffing experiments show that detached operation leads easily to X-point MARFES, impure plasmas, degradation in confinement, and lower helium pressure at the exhaust. The concept of the Lithium Vapor Box Divertor is to use local evaporation and strong differential pumping through condensation to localize the gas-phase material that absorbs the plasma heat flux and so avoid these difficulties. We use ADAS calculations of  $\epsilon_{cool}$ , the plasma energy lost per injected lithium atom, to estimate the lithium vapor pressure, and so temperature, required for detachment, taking into account power balance. We also develop a simple model of near-detachment to evaluate the required upstream density, based on further taking into account dynamic pressure balance. A remarkable general result is found, not just for lithium-induced detachment, that the upstream density divided by the Greenwald-limit density scales as  $(P^{5/8}/B^{3/8}) T_{det}/(\epsilon_{cool} + \gamma T_{det})$ , with no explicit size scaling.  $T_{det}$  is the temperature just before strong pressure loss,  $\sim 1/2$  of the ionization potential of the dominant recycling species, and  $\gamma$  is the radiational heat transmission factor.

### 1. The Challenge

The heat flux and target electron temperature in an affordable fusion power plant are likely to be higher than acceptable in standard “attached,” or even “partially attached” divertor operation. However hydrogenic and impurity puffing experiments show that detached operation leads easily to X-point MARFES, impure plasmas, degradation in confinement, and lower helium pressure at the exhaust. In the absence of a validated understanding of detachment, or scaling results as a function of heating power, it is not even clear whether naturally detached solutions exist below the Greenwald limit at the very much higher parallel and poloidal heat fluxes anticipated in a future fusion power system.

### 2. The Lithium Vapor Box Divertor

The concept behind the Lithium Vapor Box Divertor<sup>1</sup> is to control the location and density of the gas-phase material that absorbs the plasma heat flux. It uses local evaporation and strong differential pumping through condensation, as illustrated in figure 1, rather than allowing this to occur “naturally” through recycling of fuel gas and injected impurities. The configuration contains lithium vapor with margin in  $nl$  along the divertor plasma to extinguish the maximum expected heat flux. Its bottom can be wetted with a layer of lithium to handle the highest transient heat fluxes. The upper boxes are much cooler than the bottom box, so lithium is redeposited there, greatly limiting the lithium efflux to the plasma. The required flow and inventory of lithium is modest, so can be supplied to thin layers of capillary porous material along the surfaces, while some of the recirculating flow is extracted for purification.

This configuration should

- 1) avoid instability to X-point MARFE formation, since as the detachment front moves towards the vapor-box entrance the lithium vapor density falls strongly.
- 2) provide control over heat extraction from the plasma as a function of position along the divertor leg.
- 3) provide an efficient pump for impurities. Top boxes can be set to pump hydrogenics, possibly He.
- 4) be robust to changes in operating point. May tolerate ELMs, obviating the need for complex ELM-control coils that may not be practicable in a fusion reactor.

In recent work we have used Navier-Stokes calculations to confirm the estimates in [1] of the strong differential pumping capabilities of this system. We have found that reflecting surfaces must be included to induce standing shocks slowing the flow. The approximate condition for this is

$$n_{eq}(T_R)\sqrt{T_R} > n_{vap}\sqrt{T_{vap}} \quad \text{eq. 1}$$

where the subscript “*eq*” indicates the equilibrium lithium vapor pressure as a function of temperature, “*R*” indicates the reflecting surface, and “*vap*” indicates vapor quantities. Under these conditions, which should be straightforward to obtain because  $n_{vap}$  is always less than  $n_{eq}(T_{vap})$ , lithium will not be deposited on the reflector surface, and the normal flow to the surface will be halted. Figure 2 shows the falling lithium density in a model Navier-Stokes calculation with reflecting surfaces.

### 3. Power Balance

It is interesting to estimate the lithium vapor density required to extract a given amount of energy from the electron fluid in the plasma. Some of this energy is committed to ionization of the lithium, and some is lost through line and continuum radiation. (Some of the ionization energy will be returned to the electron fluid downstream, on recombination.) In our collisional-radiative model, as opposed to a pure coronal model, we used ADAS data to take into account nonlinear density effects including multi-step ionization, three-body recombination and collisional de-excitation. In order to approximate the realistic case where lithium has a finite residence time, we introduce neutral lithium as a source term in a charge-state model that includes a finite depletion time constant,  $\tau_z$ , equal for all charge states, and calculate the cooling power density, whose units are  $\text{W}/\text{m}^3$ . Dividing this result by the particle source term ( $\#/s \text{ m}^3$ ) provides a cooling energy per particle,  $\epsilon_{cool}$ , as a function of  $T_e$ ,  $n_e$ , and  $\tau_z$ , as shown in figure 3. Because of the role of 3-body interactions,  $\epsilon_{cool}$  depends on  $n_e$ , and  $\tau_z$  independently, not only in the combination  $n_e\tau_z$ . Considering the likely range of flow speeds of the lithium, and distance along B, we generally expect  $10 \mu\text{sec} < \tau_z < 1 \text{ msec}$ . The longer times are associated with the higher temperatures.

These figures suggest cooling of order a few 100 eV per particle, mostly in the form of radiation, when the electron temperature is above about 30 eV, and about 10 eV per particle, mostly in the form of ionization, at significantly lower temperatures. However, based on a two-point model even with very high radiated power, an outer mid-plane SOL temperature of at least 200 eV should be expected in ITER, and of order 300 eV in a fusion power system. In this situation, the solution to the Spitzer conductivity equation with constant radiated power loss per unit length has more than 95% of the radiated power in the region with  $T_e > 30 \text{ eV}$ .

If we assume that lithium vapor enters the divertor plasma from both sides at the Langmuir flow rate,  $n\bar{v}/4$ , and exits through the apertures shown in figure 1 with choked sonic flow, we can calculate both electron cooling and vapor efflux as functions of vapor temperature in the bottom-most box:

$$\frac{P_{dis}}{R\ell_{p,box}\varepsilon_{cool,eV}} = \frac{\dot{M}}{5.62 \cdot 10^{-8} Rd} = 4\pi en_{eq}(T_{vap})\sqrt{T_{vap}/(2\pi m)} \quad \text{eq. 2}$$

where  $P_{dis}$  is the power dissipated in a vapor box,  $\ell_{p,box}$  is the poloidal extent of the box,  $\dot{M}$  is the exit mass flow rate, and  $d$  is the exit aperture width. This is illustrated in figure 4.

#### 4. Upstream Density for Detachment

The physics of detachment is not fully understood, and even empirical scaling studies are not in hand to project the crucial dependence of the required upstream  $n/n_{GW}$  on, inter alia, divertor power, machine size, and toroidal and poloidal field strengths for simple hydrogenic gas puffing (but see A.W. Leonard et al., this issue, for a good start). Here we resort to the tactic of assuming, based on observation, that detachment takes place soon after the target temperature drops to  $T_{det} \sim 1/2$  of the dominant species ionization potential, while still maintaining dynamic pressure balance to this point. We use the standard 2-point model, extended<sup>2</sup> to take into account  $\varepsilon_{cool}$ , to find the upstream density needed to reach  $T_{det}$ .

For power balance we require,

$$\dot{N}e(\varepsilon_{cool,eV} + \gamma T_{det,eV}) = P_{div} \quad \text{eq. 3}$$

where  $\dot{N}$  represents the total recycling source of hydrogenics or lithium and  $P_{div}$  is the power flowing into the divertor leg. For particle balance (assuming that the recycling source dominates, and  $M = 1$  at the target) we require

$$\dot{N} = n_{det} \left(2eT_{det,eV}/m_i\right)^{1/2} 2\pi R_{OMP} \lambda_{\Gamma,OMP} \left(B_p/B\right)_{OMP} \quad \text{eq. 4}$$

where is the particle flux width mapped to the outer mid-plane and  $n_{det}$  is the density at the target when  $T = T_{det}$ . Substituting  $\dot{N}$  from equation 4 into equation 3, and solving for  $n_{det}$ , we have

$$n_{det} = \frac{P_{div}}{e(\varepsilon_{cool,eV} + \gamma T_{det,eV})} \left(\frac{m_i}{2eT_{det,eV}}\right)^{1/2} \left[2\pi R_{OMP} \lambda_{\Gamma,OMP} \left(B_p/B\right)_{OMP}\right]^{-1} \quad \text{eq. 5}$$

Next we use the Heuristic Drift (HD) model<sup>3</sup> for the heat flux width, with a factor of 0.8 decrease to account for the best fit to the dataset reported by Eich<sup>4</sup>, and a factor of 2 increase for diffusive spreading (S) below the X-point,  $\lambda_{int} \sim 2\lambda_q$ , based on the same dataset. We then use Spitzer conductivity to determine the upstream temperature, and assume dynamic pressure balance between up and down stream, giving

$$n_{up} = \left(\frac{2}{7} K_{0e}\right)^{2/7} \frac{(2m_i)^{1/2}}{e^{3/2}} \left(\frac{\lambda_{int,OMP}}{\lambda_{\Gamma,OMP}}\right) \left(\frac{P_{div} (B/B_p)_{OMP}}{2\pi R_{OMP} \lambda_{int,OMP}}\right)^{5/7} \left(\frac{1}{L_{det}}\right)^{2/7} \frac{T_{det,eV}^{1/2}}{(\varepsilon_{cool,eV} + \gamma T_{det,eV})} \quad \text{eq. 6}$$

where

$$\lambda_{int,OMP} = 1.6 \cdot 5671 \cdot P_{div}^{1/8} \frac{(1 + \kappa^2)^{5/8} a^{17/8} B^{1/4}}{I_p^{9/8} R} \left( \frac{2\bar{A}}{\bar{Z}^2(1 + \bar{Z})} \right)^{7/16} \left( \frac{Z_{eff} + 4}{5} \right)^{1/8} \frac{R \langle B_p \rangle}{(R + a) B_{p,OMP}} \quad \text{eq. 7}$$

The scaling of  $n_{up}/n_{GW}$  at fixed shape and aspect ratio is

$$\frac{n_{up}}{n_{GW}} \propto \frac{P_{div}^{5/8} B_T^{1/4}}{B_p^{5/8}} \frac{T_{det}}{\varepsilon_{cool} + \gamma T_{det}} \quad \text{eq. 8}$$

This is consistent with the result in a related 1-D analysis<sup>5</sup> which shows in its figure 4 that, for constant  $B$  and scrape-off width as well as  $P_{div} \propto R$ ,  $n_{up}$  is approximately proportional to  $R^{-0.3}$  and so, under these constraints,  $n_{up}/n_{GW}$  scales about as  $P_{div}^{0.7}$ . As shown in Table 1 the values are reasonable for present experiments and the projection for the lithium vapor box is promising.

The absence of any explicit size scaling in equation 8 is troubling, since the upstream SOL density clearly cannot exceed the core density. Furthermore, detailed SOL measurements on AUG<sup>6</sup> show that  $\eta_e \sim 1.4$  in the SOL as well as in the pedestal gradient region. If the SOL density approaches the Greenwald limit, and the SOL temperature is only a factor  $\sim 2$  above present experiments, this could severely restrict the achievable pedestal top temperature.

As an aside, the observation of constant  $\eta_e$  on AUG suggests a physical mechanism, such as ETG modes, that couples the SOL electron thermal heat flux channel, through the  $T_e$  profile, to the density profile. This coupling is an essential feature of the HD model.

### Future Plans

We plan to model vapor transport using the Direct Simulation Monte-Carlo package available in OpenFOAM, which allows flow studies with arbitrary collisionality. We will examine a reactor implementation, an implementation in NSTX-U, and a bench simulation experiment using steam as the working vapor. In parallel with the simulation experiment, measurements on NSTX-U should permit studies of lithium  $\varepsilon_{cool}$  and its dependencies.

This work supported by DOE Contract No. DE-AC02-09CH11466.

<sup>1</sup>R.J. Goldston, R. Myers, J. Schwartz, The Lithium Vapor Box Divertor, Phys. Scr. **T167** (2016) 014017

<sup>2</sup>P.C. Stangeby, The Plasma Boundary of Magnetic Fusion Devices, section 5.5, IOP Publishing, Bristol UK, 2000

<sup>3</sup>R.J. Goldston, Heuristic drift-based model of the power scrape-off width in low-gas-puff H-mode Tokamaks, Nucl. Fusion **52** (2012) 013009

<sup>4</sup>T. Eich et al., Scaling of the tokamak near scrape-off layer H-mode power width and implications for ITER, Nucl. Fusion **53** (2013) 093031

<sup>5</sup>A. Kallenbach et al., Analytical calculations for impurity seeded partially detached divertor conditions, Plasma Phys. Control. Fusion **58** (2016) 045013

<sup>6</sup>H.J. Sun et al., Study of near scrape-off layer (SOL) temperature and density gradient lengths with Thomson Scattering, Plasma Phys. Control. Fusion **57** (2015) 125011

Figures:

Figure 1: Poloidal cross-section of lithium vapor box divertor.

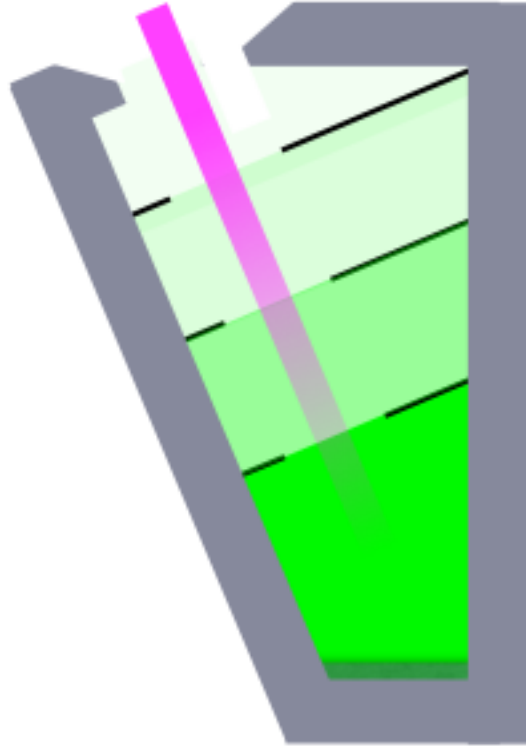


Figure 2: Navier-Stokes calculation of number density and Mach number. White apertures are assumed reflecting.

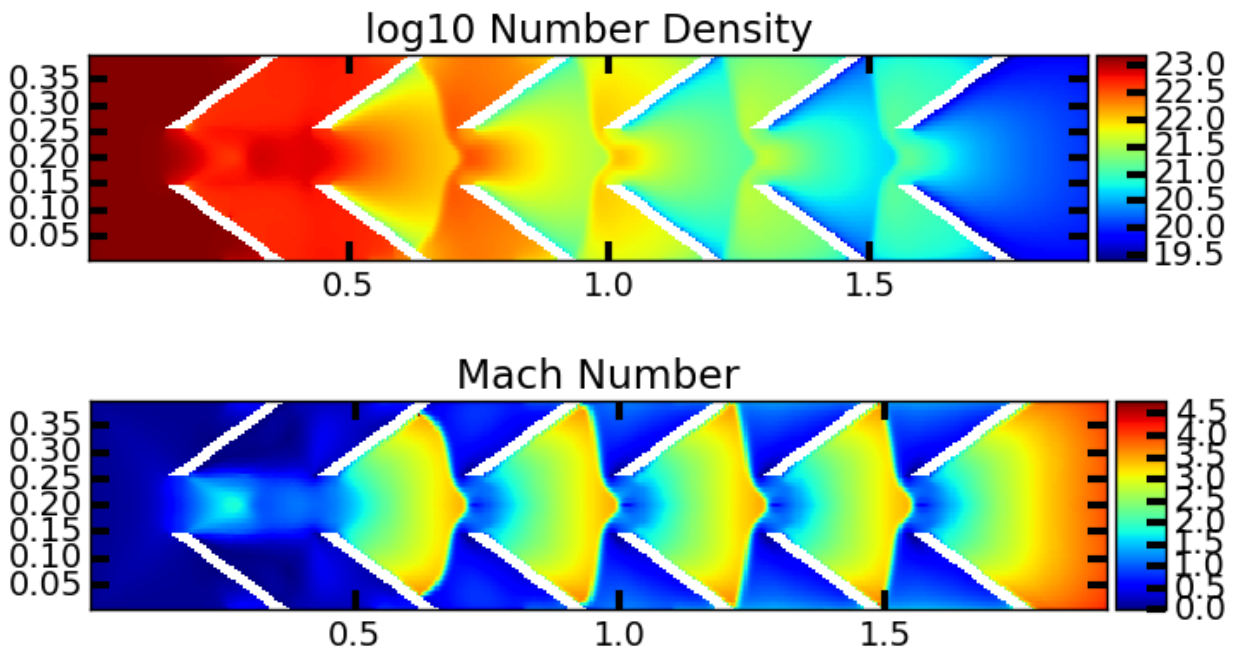




Figure 3b:  $\epsilon_{cool}$  as a function of electron temperature and density. Dashed lines are radiation-only.  $\tau_z = 100 \mu\text{sec}$ .

- $n_e = 10^{21.5}/\text{m}^3$
- $n_e = 10^{21}/\text{m}^3$
- $n_e = 10^{20.5}/\text{m}^3$
- $n_e = 10^{20}/\text{m}^3$
- $n_e = 10^{19.5}/\text{m}^3$
- $n_e = 10^{19}/\text{m}^3$

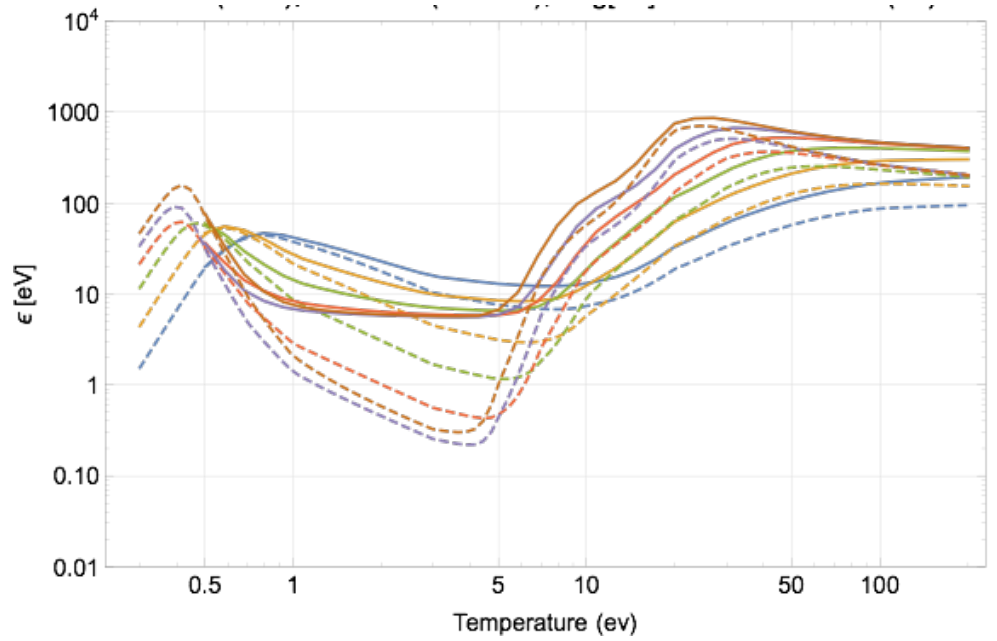


Figure 3c:  $\epsilon_{cool}$  as a function of electron temperature and density. Dashed lines are radiation-only.  $\tau_z = 1$  msec.

- $n_e = 10^{21.5}/\text{m}^3$
- $n_e = 10^{21}/\text{m}^3$
- $n_e = 10^{20.5}/\text{m}^3$
- $n_e = 10^{20}/\text{m}^3$
- $n_e = 10^{19.5}/\text{m}^3$
- $n_e = 10^{19}/\text{m}^3$

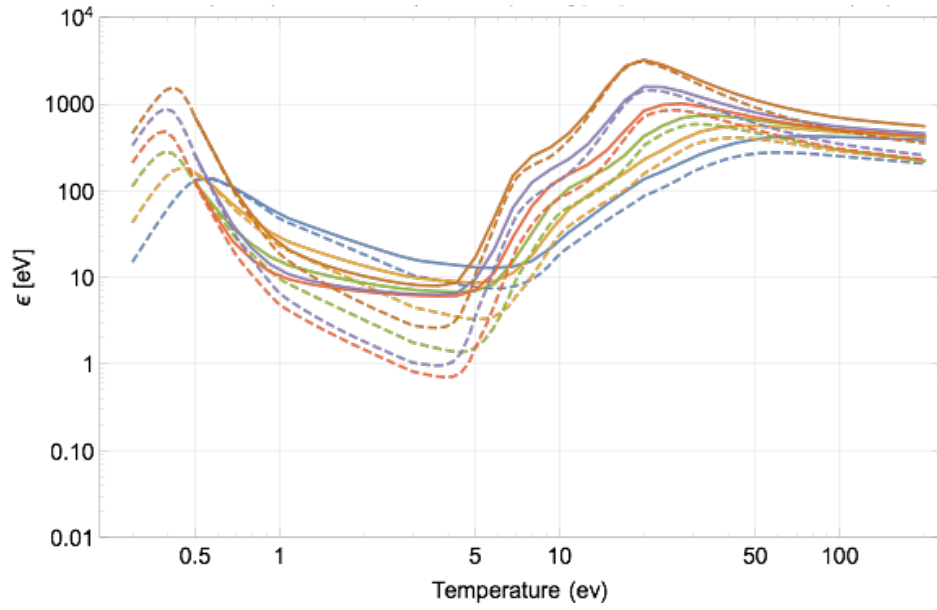
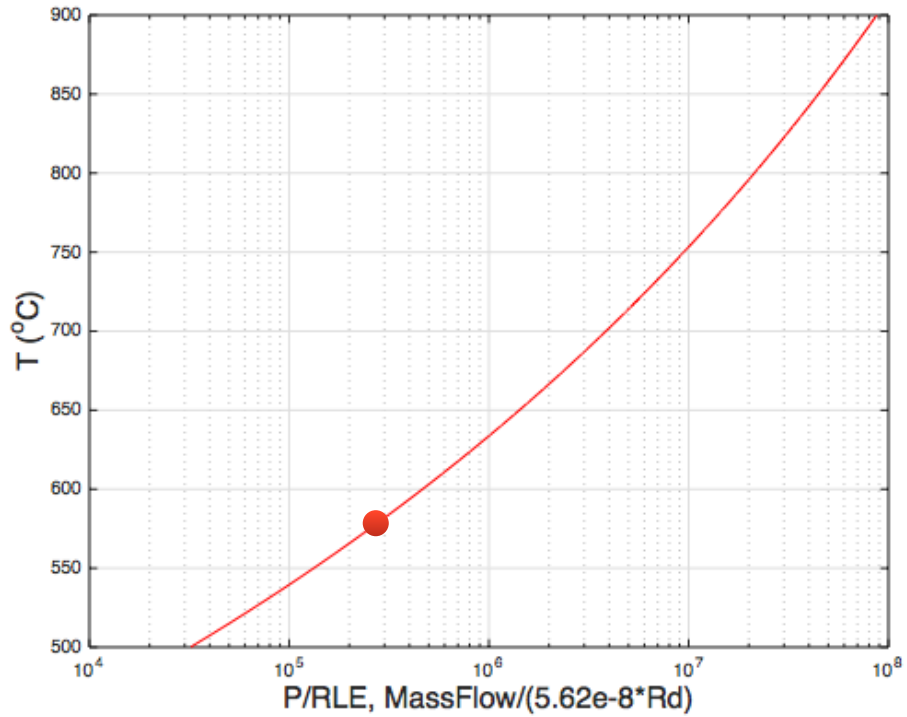


Figure 4: Vapor temperature as a function of required dissipation power, with resulting mass efflux. For example 200 MW of dissipated power, with  $R = 6\text{m}$ ,  $l_{p, box} = 0.5\text{m}$  and  $\epsilon_{cool} = 250$  eV gives about  $580\text{ }^\circ\text{C}$ . The mass efflux through a 20cm aperture would be  $18\text{g/s}$ . This could easily be differentially pumped to much less than  $1\text{g/s}$ . Much lower values of  $\epsilon_{cool}$  clearly can also be accommodated.



## LaTeX for equations

1. 
$$\left[ n_{\text{eq}} \left( T_{\text{R}} \right) \sqrt{T_{\text{R}}} > n_{\text{vap}} \sqrt{T_{\text{vap}}} \right]$$
2. 
$$\frac{P_{\text{dis}}}{R \ell_{\text{p,box}} \varepsilon_{\text{cool,eV}}} = \frac{\dot{M}}{5.62 \cdot 10^{-8} \text{Rd}} = 4\pi e_{\text{eq}} \left( T_{\text{vap}} \right) \sqrt{T_{\text{vap}}} \left( 2\pi m \right)$$
3. 
$$\dot{N} \left( \varepsilon_{\text{cool,eV}} + \gamma T_{\text{det,eV}} \right) = P_{\text{div}}$$
4. 
$$\dot{N} = n_{\text{det}} \left( 2e T_{\text{det,eV}} \mathop{\leftarrow} \left[ \vphantom{2e T_{\text{det,eV}}} m_i \right] \right)^{1/2} 2\pi R_{\text{OMP}} \lambda_{\text{Gamma,OMP}} \left( B_p \mathop{\leftarrow} \left[ \vphantom{B_p} B \right] \right)_{\text{OMP}}$$
5. 
$$n_{\text{det}} = \frac{P_{\text{div}}}{e \left( \varepsilon_{\text{cool,eV}} + \gamma T_{\text{det,eV}} \right) \left( \frac{m_i}{2e T_{\text{det,eV}}} \right)^{1/2} \left[ 2\pi R_{\text{OMP}} \lambda_{\text{Gamma,OMP}} \left( B_p \mathop{\leftarrow} \left[ \vphantom{B_p} B \right] \right)_{\text{OMP}} \right]^{-1}}$$
6. 
$$n_{\text{up}} = \left( \frac{2}{7} \kappa_{0e} \right)^2 \mathop{\leftarrow} \left[ \vphantom{2/7} 7 \right] \frac{\left( \frac{m_i}{2} \right)^{1/2} e^{3/2} \left( \frac{\lambda_{\text{int,OMP}}}{\lambda_{\text{Gamma,OMP}}} \right) \left( \frac{P_{\text{div}}}{B_p \mathop{\leftarrow} \left[ \vphantom{B_p} B \right]} \right)_{\text{OMP}}}{2\pi R_{\text{OMP}} \lambda_{\text{int,OMP}}} \left( \frac{1}{L_{\text{det}}} \right) \left( T_{\text{det,eV}} \right)^{2/7} \frac{T_{\text{det,eV}}^{1/2}}{\left( \varepsilon_{\text{cool,eV}} + \gamma T_{\text{det,eV}} \right)}$$
7. 
$$\lambda_{\text{int,OMP}} = 1.6 \cdot 5671 \cdot P_{\text{div}}^{1/8} \frac{\left( 1 + \kappa^2 \right)^{5/8} a^{17/8} B^{1/4} I_p^{9/8} R}{\left( \frac{2\bar{A}}{\bar{Z}^2} \left( 1 + \bar{Z} \right) \right) \left( \frac{Z_{\text{eff}}}{4} \right)^5 \left( R + a \right) B_{\text{p,OMP}}}$$
8. 
$$\frac{P_{\text{div}}^{5/8} B_T^{1/4}}{B_p^{5/8}} \frac{1}{T_{\text{det}} \varepsilon_{\text{cool}} + \gamma T_{\text{det}}}$$

Table

Table 1: Projected upstream densities for nominal DIII-D, JET, ITER and Demo parameters. Demo is presumed to be geometrically similar to ITER, but operating at 7T and producing 2.5 GW(th) at  $Q = 25$ . Hydrogenic cooling on the left, Li cooling on the right.

	DIII-D (DD)	JET (DD)	ITER (DT)	Demo (DT)	DIII-D (Li)	JET (Li)	ITER (Li)	Demo (Li)
<b>R</b>	1.65	3	6.2	6.2	1.65	3	6.2	6.2
<b>a</b>	0.6	0.85	2	2	0.6	0.85	2	2
<b>B</b>	1.6	2.5	5	7	1.6	2.5	5	7
<b>I<sub>p</sub></b>	9E+05	2.5E+06	1.5E+07	2.1E+07	9E+05	2.5E+06	1.5E+07	2.1E+07
<b>&lt;B<sub>p</sub>&gt;</b>	0.206	0.404	1.030	1.442	0.206	0.404	1.030	1.442
<b>P<sub>div</sub></b>	1.7E+06	8E+06	5E+07	2E+08	1.7E+06	8E+06	5.0E+07	2E+08
<b>L<sub>det</sub></b>	1.56E+01	2.83E+01	5.84E+01	5.84E+01	1.56E+01	2.83E+01	5.84E+01	5.84E+01
<b>A<sub>i</sub></b>	2.00E+00	2.00E+00	2.50E+00	2.50E+00	6.90E+00	6.90E+00	6.90E+00	6.90E+00
<b>T<sub>det, eV</sub></b>	6.80E+00	6.80E+00	6.80E+00	6.80E+00	2.70E+00	2.70E+00	2.70E+00	2.70E+00
<b>λ<sub>ini</sub>/λ<sub>r</sub></b>	5.00E-01	5.00E-01	5.00E-01	5.00E-01	5.00E-01	5.00E-01	5.00E-01	5.00E-01
<b>ε<sub>cool, eV</sub></b>	3.00E+01	3.00E+01	3.00E+01	3.00E+01	2.50E+02	2.50E+02	2.50E+02	2.50E+02
<b>n<sub>up</sub></b>	3.22E+19	7.84E+19	1.75E+20	5.13E+20	7.66E+18	1.87E+19	3.99E+19	1.17E+20
<b>n<sub>up</sub>/n<sub>GW</sub></b>	4.04E-01	7.12E-01	1.47E+00	3.07E+00	9.63E-02	1.70E-01	3.35E-01	7.01E-01

# Princeton Plasma Physics Laboratory Office of Reports and Publications

Managed by  
Princeton University

under contract with the  
U.S. Department of Energy  
(DE-AC02-09CH11466)

---

P.O. Box 451, Princeton, NJ 08543  
Phone: 609-243-2245  
Fax: 609-243-2751

E-mail: [publications@pppl.gov](mailto:publications@pppl.gov)

Website: <http://www.pppl.gov>